International Orthopaedics (2018) 42:2329–2334
https://doi.org/10.1007/s00264-018-3843-9

ORIGINAL PAPER

The tridimensional geometry of the proximal femur should determine the design of cementless femoral stem in total hip arthroplasty

Julien Wegrzyn[1,2] · Jean-Paul Roux[2] · Charlotte Loriau[2] · Nicolas Bonin[3] · Vincent Pibarot[1]

Received: 18 November 2017 / Accepted: 11 February 2018 / Published online: 22 February 2018

Abstract

Purpose Using a cementless femoral stem in total hip arthroplasty (THA), optimal filling of the proximal femoral metaphyseal volume (PFMV) and restoration of the extramedullary proximal femoral (PF) parameters (i.e., femoral offset (FO), neck length (FNL), and head height (FHH)) constitute key goals for optimal hip biomechanics, functional outcome, and THA survivorship. However, almost 30% of mismatch between the PF anatomy and implant geometry of the most widely implanted non-modular cementless femoral stem has been demonstrated in a computed tomography scan (CT scan) study. Therefore, this anatomic study aimed to evaluate the relationship between the intra- and extramedullary PF parameters using tridimensional CT scan reconstructions.

Methods One hundred fifty-one CT scans of adult healthy hips were obtained from 151 male Caucasian patients (mean age = 66 ± 11 years) undergoing lower limb CT scan arteriography. Tridimensional PF reconstructions and parameter measurements were performed using a corrected PF coronal plane—defined by the femoral neck and diaphyseal canal longitudinal axes—to avoid influence of PF helitorsion and femoral neck version on extramedullary PF parameters.

Results Independently of the femoral neck-shaft angle, the PFMV was significantly and positively correlated with the FO, FNL, and FHH ($r = 0.407$ to 0.420; $p < 0.0001$).

Conclusion This study emphasized that the tridimensional PF geometry measurement in the corrected coronal plane of the femoral neck can be useful to determine and optimize the design of a non-modular cementless femoral stem. Particularly, continuous homothetic size progression of the intra- and extramedullary PF parameters should be achieved to assure stem fixation and restore anatomic hip biomechanics.

Keywords Total hip arthroplasty · Cementless femoral stem · Proximal femur · Tridimensional anatomy · Computed tomography

Introduction

Using a non-modular cementless femoral stem in total hip arthroplasty (THA), optimal filling of the proximal femoral metaphyseal volume (PFMV) improves implant primary stability, mechanical stress transmission to the bone, bone ingrowth ability, and then durable secondary biologic fixation [1–6]. In addition, restoration of the extramedullary proximal femoral (PF) parameters such as femoral offset (FO), neck length (FNL), and head height (FHH) constitutes key goals to achieve for optimal hip biomechanics and avoiding leg length discrepancy [7–14]. Particularly, FO restoration has been demonstrated to improve hip abductor mechanism function while preventing gait alterations, instability, and wear after THA [7–14]. Therefore, restoring the extramedullary PF anatomy is critical for THA outcome along with an accurate PF endosteal stem filling. This poses a challenge as the PF anatomy represents a complex tridimensional (3D) geometry. However, most of the commercially available non-modular cementless femoral stem designs are limited in their potential to adjust simultaneously the extra- and intramedullary PF parameters intra-operatively [12, 15]. For example, in a computed tomography (CT) scan study, Boese CK et al. [15] demonstrated almost 30% of mismatch between the extramedullary

✉ Julien Wegrzyn
julien.wegrzyn@chu-lyon.fr

[1] Department of Orthopedic Surgery – Pavillon T, Hospices Civils de Lyon, Hôpital Edouard Herriot, 5, place d'Arsonval, 69437 Lyon, France

[2] INSERM UMR 1033, Université de Lyon, Lyon, France

[3] Lyon-Ortho-Clinic, Clinique de la Sauvegarde, Lyon, France

PF anatomy of adult hips and implant geometry of the most widely implanted non-modular cementless femoral stem. In this way, using CT scan assessment of the hip anatomy, some authors argued that the current commercially available non-modular cementless stems may not be able to restore anatomy of the hip joint and therefore advocated the use of custom-made or modular neck femoral stems [16, 17].

The wide majority of the non-modular cementless stems have been designed using two-dimensional (2D) anatomic evaluation of this complex 3D PF geometry performed on conventional antero-posterior (AP) and lateral radiographs of the hip [18]. Significant errors in the measurement of the FO or femoral neck-shaft angle have been described with 2D AP radiographic projection of the PF when compared to their measurements using CT scan coronal reconstruction of the PF in the femoral neck plane [3–7, 15–17, 19]. In addition, previous anatomic studies tended to demonstrate that the intra- and extramedullary PF parameters were independent, supporting the use of non-homothetic femoral stem regarding the size progression of the intra- and extramedullary PF geometry [3, 6, 18]. However, these studies, rather than measuring the PFMV, were based on the assessment of the canal flare index (CFI) which represents the intramedullary morphology of the 2D AP projection of the PF in the coronal plane [1–6].

Therefore, the current anatomic study aimed to evaluate the relationship between the intra- and extramedullary PF parameters using 3D CT scan reconstructions of adult healthy hips in a corrected coronal plane. We hypothesized that a continuous homothetic size progression of the intra- and extramedullary PF parameters should be achieved when designing a non-modular cementless femoral stem in order to assure the restoration of the extramedullary PF geometry along with an optimal filling of the endomedullary volume.

Material and methods

A retrospective series of 151 CT scans of left adult healthy hips including the whole pelvis and femur was obtained from 151 male Caucasian patients (mean age = 66 ± 11 years) undergoing lower limb CT scan arteriography. These 151 CT scans were selected into the database of the Department of Radiology at our institution by a senior radiologist specialized in musculoskeletal imaging. The exclusion criteria were patients with prior fracture or surgery of the acetabulum or femur, hip osteoarthritis, rheumatism, dysplasia or deformity, or bone diseases. Image acquisitions were performed using a Philips Ingenuity® 128-slice CT scan (Philips Healthcare, Eindhoven, The Netherlands) operating with the following parameters: X-ray source = 120 kV; 164 mA, collimation = 64 × 0.625 mm, field of view = 400 mm, resolution = 512 × 512 pixels, slice thickness = 1.50 mm, and slice increment = 0.75 mm. All the CT scans were selected and extracted anonymously in a DICOM format. Inclusion and exclusion criteria were checked by a senior orthopaedic surgeon not involved in the current study. Owing to French regulation, IRB approval and patient informed consent were not required to conduct this study.

The 3D PF reconstructions were performed from the femoral head to the mid-diaphysis isthmus using InVesalius 3 Beta 4® software (CTI Renato Archer, Sao Paulo, Brazil). The trabecular bone was subtracted from the 3D PF reconstructions using grayscale thresholds set at 662 to 1988 Hounsfield units (HU) for cortical bone and 148 to 661 HU for trabecular bone [20]. Then, these reconstructions were exported to PTC Creo Elements/Pro 5.0® software (PTC Inc., Needham, MA, USA) for image analyses and parameter measurements. The center of the femoral head (C) was defined as the centre of a perfect sphere filling and fitting the femoral head volume. The femoral neck longitudinal axis was defined as the longitudinal axis of a perfect cylinder filling and fitting the femoral neck volume starting from C. A corrected PF coronal plane was defined as the plane subtended by the femoral neck longitudinal axis and the centre of the femoral diaphyseal canal at 120 mm from C. This corrected PF coronal plane was used in order to avoid influence of PF helitorsion and femoral neck version on the extramedullary PF parameter measurements [3–5]. Then, using this corrected PF coronal plane, the femoral diaphyseal canal longitudinal axis (D) was defined by three points representing the centre of the diaphyseal canal at 50, 90, and 120 mm from C. The caput–column–diaphyseal angle (CC′D angle or femoral neck-shaft angle) was defined as the angle subtended by the longitudinal axes of the femoral neck (CC′) and the femoral diaphyseal canal (C′D) with C′ representing the intersection point between these two axes (Fig. 1). The CC′D angle evaluated the hip morphology (i.e., coxa vara < 120°, coxa norma = [120°–135°] and coxa valga > 135°) [21]. The extramedullary PF parameters corresponded to a right triangle with the femoral neck length (FNL) corresponding to the hypotenuse (i.e., [CC′]), the femoral offset (FO) the opposite, and the femoral head height (FHH) the adjacent (Fig. 1). The FO, FNL, and FHH were measured in millimeters. The intramedullary PF parameter corresponded to the proximal femoral metaphyseal volume (PFMV) defined by the volume of the proximal metaphysis between 50 and 90 mm from C. The PFMV was measured in cubic centimeter and represented the metaphyseal press-fit fixation volume for a cementless femoral stem [22–24].

The 3D PF reconstructions and parameter measurements were performed by a single senior surgeon not involved in the CT scan selection process. The intra-observer reproducibility in measurements of the intra- and extramedullary PF parameters was evaluated on 50 randomly selected 3D PF reconstructions at a time interval of 1 month using single-measure intra-class correlation coefficients (ICCs) using

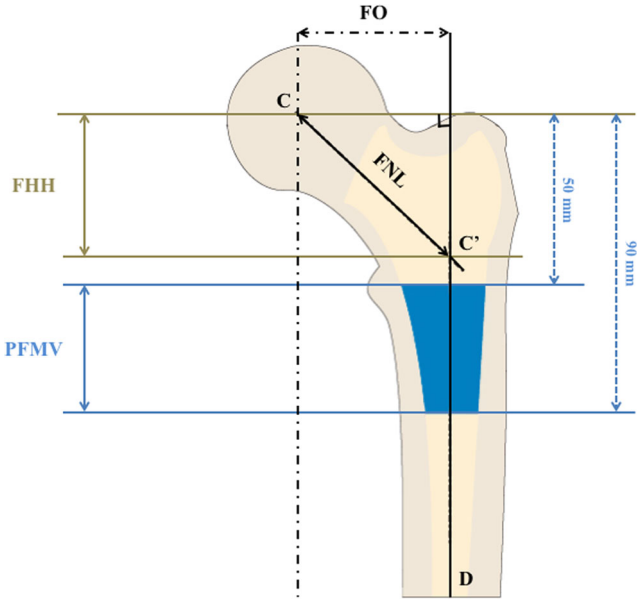

Fig. 1 Schematic representation of the intra- and extramedullary proximal femoral parameters. PFMV proximal femoral metaphyseal volume, CC′D caput-column-diaphyseal or femoral neck-shaft angle, FNL femoral neck length, FO femoral offset, FHH femoral head height, C femoral head centre, D femoral diaphyseal canal longitudinal axis, C′ intersection point between the femoral neck and the femoral diaphyseal canal longitudinal axes

two-way random effects model for absolute agreement. ICCs were excellent ranging from 0.94 to 0.97.

Statistical analyses

Kolmogorov-Smirnov tests were used to assess whether the variables were normally distributed. All the variables were normally distributed, except the PFMV which was normalized using logarithmic transformation. Descriptive data were presented as mean ± standard deviation (SD). Pearson's coefficients of correlation and partial linear regression analyses were used for the analysis of the relationship between two continuous variables. Statistical analyses were performed using IBM SPSS Statistics 22.0 (IBM Corp. Armonk, NY, USA) with a level of significance set at $p < 0.05$.

Results

Descriptive statistics are reported in Table 1. The PFMV was significantly and positively correlated with the FO, FNL, FNH, and CC′D angle ($r = 0.223$ to 0.638; $p < 0.0001$ to 0.001) (Table 2). In addition, the extramedullary PF parameters were significantly and positively correlated altogether ($|r| = 0.224$ to 0.828; $p < 0.0001$ to 0.001) (Table 2).

After adjustment for CC′D angle, the correlations between the PFMV and the extramedullary PF parameters remained significant ($r = 0.407$ to 0.420; $p < 0.0001$) as well as the correlation between the three extramedullary PF parameters ($r = 0.986$ to 0.997; $p < 0.0001$) (Table 3) (Fig. 2a–c). In addition, FO increased 0.7 mm, FNL increased 0.8 mm, and FHH increased 0.4 mm for each cubic centimeter of increase in PFMV, with the PFMV ranging from 2 to 20 cm^3 ($p < 0.0001$) (Fig. 2a–c).

Table 1 Descriptive statistics of the intra- and extramedullary proximal femoral parameters. *CC′D angle* caput–column–diaphyseal or femoral neck-shaft angle

	Mean ± SD
Femoral offset (mm)	45 ± 5
Femoral neck length (mm)	56 ± 6
Femoral head height (mm)	32 ± 5
CC′D angle (°)	126 ± 5
Proximal femoral metaphyseal volume (cm^3)	10 ± 3

Discussion

The most important finding of the current anatomic study was that the intra- and extramedullary PF parameters were significantly and positively correlated when measured using 3D CT scan reconstruction of the PF in a corrected coronal plane. In addition, our results demonstrated a linear progression between the PFMV and the extramedullary PF geometry independently of the hip morphology, i.e., coxa norma, valga, or vara. When using a non-modular cementless femoral stem during THA, the optimal component should allow both optimal endosteal stem filling and individual restoration of anatomic hip biomechanics [3–6, 8–14]. This poses a challenge to the surgeon as the PF anatomy represents a complex 3D geometry. Most of the commercially available non-modular cementless femoral stem designs are limited in their potential

Table 2 Pearson's coefficients of correlation (r) among the intra- and extramedullary proximal femoral parameters. *CC′D angle* caput–column–diaphyseal or femoral neck-shaft angle

	Femoral offset	Femoral neck length	Femoral head height	CC′D angle
Femoral neck length	$r = 0.828$ $p < 0.0001$			
Femoral head height	$r = 0.232$ $p = 0.001$	$r = 0.734$ $p < 0.0001$		
CC′D angle	$r = -0.354$ $p < 0.0001$	$r = 0.224$ $p = 0.001$	$r = 0.821$ $p < 0.0001$	
Proximal femoral metaphyseal volume	$r = 0.223$ $p = 0.001$	$r = 0.528$ $p < 0.0001$	$r = 0.638$ $p < 0.0001$	$r = 0.481$ $p < 0.0001$

Table 3 Pearson's coefficients of correlation (r) among the intra- and extramedullary proximal femoral parameters after adjustment for CC′D angle. *CC'D angle* caput–column–diaphyseal or femoral neck-shaft angle

Adjustment for CC′D angle	Femoral offset	Femoral neck length	Femoral head height
Femoral neck length	$r = 0.997$ $p < 0.0001$		
Femoral head height	$r = 0.986$ $p < 0.0001$	$r = 0.993$ $p < 0.0001$	
Proximal femoral metaphyseal volume	$r = 0.408$ $p < 0.0001$	$r = 0.420$ $p < 0.0001$	$r = 0.407$ $p < 0.0001$

to adjust simultaneously the extra- and intramedullary PF geometry intra-operatively [12, 15]. With a survivorship of 94% at a 30-year follow-up, the Corail® stem system (DePuy Synthes, Warsaw, IN, USA) represents the most widely implanted and reproduced non-modular cementless femoral stem [25, 26]. However, this stem did not offer a continuous homothetic size by size progression of the intra- and extramedullary geometry [15, 18]. Indeed, Boese CK et al. [15] have demonstrated, in a CT scan anatomic study, almost 30% of mismatch ≥ 6 mm between the extramedullary PF anatomy and the Corail® stem geometry despite its three stem shaft variants and five femoral head sizes available. Similarly, Bourne RB et al. [12] reported a FO restoration in only 40 and 68% of the THA when using a conventional non-modular cementless stem design with 135° and 131° femoral neck-shaft angles, respectively. Therefore, even with the use of lateralized femoral stems, FO may not be restored in a significant proportion of the hips [7, 12, 19]. In these cases, restoration of the extramedullary PF geometry could lead the surgeon to adjust intra-operatively the level of the femoral neck osteotomy or the head size which could in turn compromise leg length, particularly with limb lengthening causing potential patient's dissatisfaction and litigation after THA [7].

The majority of the non-modular cementless femoral stems available in routine surgical practice were initially designed using 2D measurements of the 3D PF geometry performed on conventional AP and lateral radiographs of the hip with the lower limb placed in internal rotation and the patella located at the zenith in the coronal plane. However, Rubin PJ et al. [4] demonstrated the weakness of conventional 2D radiographs for a reliable morphometric analysis of the 3D PF geometry even with the use of standardized radiographic and measurement methods. Particularly, PF helitorsion, femoral neck version, hip external rotation and flexion contracture, and patient's compliance could result in clinically relevant 2D projection errors of the 3D PF geometry in the coronal plane [3–6, 15–18]. Moreover, conventional radiographs are subjected to magnification and distortion artifacts with the radiologic enlargement proportionally distorting all the linear parameters [5, 16, 18]. Indeed, previous studies reported that measuring the extramedullary geometry using 2D AP projection of the PF resulted in an average 8% underestimation of the FO and an average 3° overestimation of the femoral neck-shaft angle when compared to their measurements performed with CT scan PF reconstruction in the corrected coronal plane of the femoral neck [13, 16, 21]. However, obtaining adequate FO restoration after THA is critical and influences THA functional outcome, stability, and survivorship [8–14]. Gait analysis and finite element analysis studies reported that a 15 to 20% decrease in FO was associated with a weakness of the abductor mechanism by reducing its lever arm, resulting in gait alterations with Trendelenburg limping and reduced impingement-free THA range of motion [11–14]. In addition, such a decrease in FO leads to increased joint reaction forces applied onto the bearing surfaces and the cup resulting in negative effects on THA wear and survivorship [11–14]. In this way, using CT scan assessment of the hip anatomy, some authors argued that the current commercially available non-modular cementless stems may not be able to restore anatomy

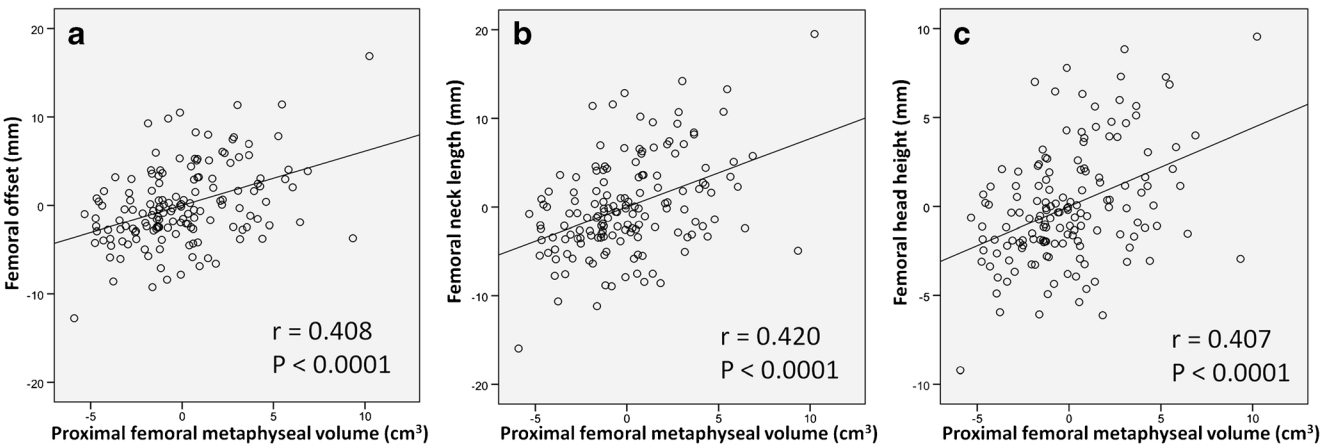

Fig. 2 Partial linear regression scatter plots between the proximal femoral metaphyseal volume and the femoral offset (**a**), neck length (**b**), and head height (**c**) after adjustment for CC′D angle

of the hip joint and therefore advocated the use of custom-made or modular neck femoral stems [16, 17]. However, custom-made femoral stems represent a time-consuming and high manufacturing cost alternative to established standard implants and their use is mostly restricted to individual particular cases [27, 28]. In addition, modular neck femoral stems have raised serious concerns regarding their mid- to long-term survivorship due to major adverse effects related to modular neck fretting corrosion and fracture, metallic wear debris generation, and acute local tissue reaction [16, 17, 29–31].

In the current study, the dimensions of the extramedullary PF parameters were similar to those reported in literature [3–6, 20]. However, to our knowledge, no previous anatomic study evaluated the intramedullary PF geometry with the measure of a 3D parameter, i.e., the PFMV. Using CFI measurements, the previous 2D anatomic studies tended to demonstrate that the intra- and extramedullary PF parameters were independent, supporting the use of non-homothetic femoral stem regarding the size progression of the intra- and extramedullary PF geometry [3, 6, 18]. The CFI, initially described by Noble PC et al. [3], categorizes the 2D AP projection of the PF according to its morphometric measurement in the coronal plane distinguishing champagne-fluted, normal, and stove-pipe canal shapes. This classification is still widely used for the design of non-modular cementless femoral stems [5]. However, similarly to the evaluation of the extramedullary parameter geometry, the CFI is not reliable for an accurate 3D evaluation of the intramedullary PF geometry and defines the PF morphology in the coronal plane only [2–6]. A close geometric filling of the intramedullary PF volume by the femoral stem is essential for a durable cementless fixation [1–6, 19, 20]. The strength and rigidity of the PF trabecular bone have been reported to increase significantly at 2 to 5 mm of the cortical wall [1–3]. Consequently, a direct intramedullary support of the femoral stem could be allowed only when the stem design closely approximates the PF endosteal volume which requires a 3D PF evaluation [20]. Therefore, demonstrating correlations between the intra- and extramedullary PF geometry, this 3D anatomic study supported the use of homothetic femoral stem in THA in order to restore the extramedullary PF geometry and hip biomechanics while ensuring an optimal endomedullary filling and cementless fixation.

The current study presented with four main limitations. First, the influence of cup placement was not evaluated to determine the optimal femoral stem FO and neck length. Particularly, cup medialization with a compensatory increase of FO has been recommended to improve THA range of motion and abductor mechanism function [32]. Second, this study evaluated the 3D PF geometry in a single cohort of male Caucasian patients. Similarly, owing to the single observer design, the inter-observer reliability assessment of the measurements was not performed. Third, the mean age of the analyzed cohort was slightly lower when compared with patients undergoing THA. Previous studies reported an age-dependent change in the PF anatomic parameters with a decrease in the femoral neck-shaft angle resulting in a subsequent increase in FO and an expansion of the intramedullary volume with a shift toward stove-pipe PF morphology [3, 33]. Fourth, the influence of femoral stem version and leg length was not taken into account in the current study as well. However, alteration in FO has been demonstrated as the worst scenario for the abductor mechanism lever arm in a finite element analysis study [14]. Nevertheless, the aim of the current study was not primarily to conceive one more prosthesis but to serve as an anatomic reference to a surgeon's selection of a non-modular cementless femoral stem with more criticism in its clinical practice. We believe that our results may contribute to the optimization of the design of future femoral stems.

Conclusion

This study emphasized that the measurement of the 3D PF geometry using CT scan reconstructions in the corrected coronal plane of the femoral neck can be useful to determine and optimize the design of a non-modular cementless femoral stem. Particularly, a continuous homothetic size progression of the femoral stem endomedullary volume and extramedullary geometry should be achieved to ensure a durable cementless fixation and to restore anatomic hip biomechanics.

Acknowledgements The authors thank the AXIOM orthopaedic group for providing assistance in CT scan selection and revision of the manuscript content.

Funding This study was internally funded by the research laboratory INSERM UMR1033, Université de Lyon, Lyon, France.

Compliance with ethical standards

Conflict of interest JPR and CL declare that they have no conflict of interest. JW, NB, and VP declare royalties perceived from Dedienne Santé, Maugio, France. JW serves as paid consultant for Stryker, Mahwah, NJ, USA.

Ethical approval All procedures performed in this study involving human participants were in accordance with the ethical standards of our institutional and the French national research committees, and with the 1964 Helsinki declaration and its later amendments or comparable ethical standards.

Informed consent As this study evaluated anonymized data issued from CT scan primarily performed for clinical purpose and not research, informed consent was not required.

References

1. Dorr LD, Faugere MC, Mackel AM, Gruen TA, Bognar B, Malluche HH (1993) Structural and cellular assessment of bone quality of proximal femur. Bone 14:231–242
2. Laine HJ, Lehto MU, Moilanen T (2000) Diversity of proximal femur medullary canal. J Arthroplast 15:86–92
3. Noble PC, Alexander JW, Lindahl LJ, Yew DT, Granberry WM, Tullos HS (1988) The anatomic basis of femoral component design. Clin Orthop Relat Res (235):148–165
4. Rubin PJ, Leyvraz PF, Aubaniac JM, Argenson JN, Estève P, de Roguin B (1992) The morphology of the proximal femur. A three-dimensional radiographic analysis. J Bone Joint Surg Br 74-B:28–32
5. Husmann O, Rubin PJ, Leyvraz PF, de Roguin B, Argenson JN (1997) Three-dimensional morphology of the proximal femur. J Arthroplast 12:444–450
6. Merle C, Waldstein W, Gregory JS, Goodyear SR, Aspden RM, Aldinger PR, Murray DW, Gill HS (2014) How many different types of femora are there in primary hip osteoarthritis? An active shape modeling study. J Orthop Res 32:413–422. https://doi.org/10.1002/jor.22518
7. Flecher X, Ollivier M, Argenson JN (2016) Lower limb length and offset in total hip arthroplasty. Orthop Traumatol Surg Res 102:S9–S20. https://doi.org/10.1016/j.otsr.2015.11.001
8. Matsushita A, Nakashima Y, Jingushi S, Yamamoto T, Kuraoka A, Iwamoto Y (2009) Effects of the femoral offset and the head size on the safe range of motion in total hip arthroplasty. J Arthroplast 24:646–651. https://doi.org/10.1016/j.arth.2008.02.008
9. McGrory BJ, Morrey BF, Cahalan TD, An KN, Cabanela ME (1995) Effects of femoral offset on range of motion and abductor muscle strength after total hip arthroplasty. J Bone Joint Surg Br 77:865–869
10. Sakalkale DP, Sharkey PF, Eng K, Hozack WJ, Rothman RH (2001) Effects of femoral component offset on polyethylene wear in total hip arthroplasty. Clin Orthop Relat Res 388:125–134
11. Asayama I, Chamnongkich S, Simpson KJ, Kinsey TL, Mahoney OM (2005) Reconstructed hip joint position and abductor muscle strength after total hip arthroplasty. J Arthroplast 20:414–420
12. Bourne RB, Rorabeck CH (2002) Soft tissue balancing: the hip. J Arthroplast 17(Suppl 1):17–22
13. Sariali E, Klouche S, Mouttet A, Pascal-Moussellard H (2014) The effect of femoral offset modification on gait after total hip arthroplasty. Acta Orthop 85:123–127. https://doi.org/10.3109/17453674.2014.889980
14. Rudiger HA, Parvex V, Terrier A (2016) Impact of the femoral head position on moment arms in total hip arthroplasty: a parametric finite element study. J Arthroplast 31:715–720. https://doi.org/10.1016/j.arth.2015.09.044
15. Boese CK, Dargel J, Jostmeier J, Eysel P, Frink M, Lechler P (2016) Agreement between proximal femoral geometry and component design in total hip arthroplasty: implications for implant choice. J Arthroplast 31(8):1842. https://doi.org/10.1016/j.arth.2016.02.015
16. Sariali E, Mouttet A, Pasquier G, Durante E (2009) Three-dimensional hip anatomy in osteoarthritis. Analysis of the femoral offset. J Arthroplasty 24:990–997. https://doi.org/10.1016/j.arth.2008.04.031
17. Sariali E, Mouttet A, Pasquier G, Durante E, Catone Y (2009) Accuracy of reconstruction of the hip using computerised three-dimensional pre-operative planning and a cementless modular neck. J Bone Joint Br 91:333–340. https://doi.org/10.1302/0301-620X.91B3.21390
18. Lecerf G, Fessy MH, Philippot R, Massin P, Giraud F, Flecher X, Girard J, Mertl P, Marchetti E, Stindel E (2009) Femoral offset: anatomical concept, definition, assessment, implications for preoperative templating and hip arthroplasty. Orthop Traumatol Surg Res 95:210–219. https://doi.org/10.1016/j.otsr.2009.03.010
19. Massin P, Geais L, Astoin E, Simondi M, Lavaste F (2000) The anatomic basis for the concept of lateralized femoral stems: a frontal plane radiographic study of the proximal femur. J Arthroplasty 15:93–101
20. Baharuddin MY, Salleh SH, Zulkifly AH, Lee MH, Noor AM, A Harris AR, Majid NA, Abd Kader AS (2014) Design process of cementless femoral stem using a nonlinear three dimensional finite element analysis. BMC Musculoskelet Disord 15:30. https://doi.org/10.1186/1471-2474-15-30
21. Boese CK, Dargel J, Oppermann J, Eysel P, Scheyerer MJ, Bredow J, Lechler P (2016) The femoral neck-shaft angle on plain radiographs: a systematic review. Skelet Radiol 45:19–28. https://doi.org/10.1007/s00256-015-2236-z
22. Issa K, Pivec R, Wuestemann T, Tatevossian T, Nevelos J, Mont MA (2014) Radiographic fit and fill analysis of a new second-generation proximally coated cementless stem compared to its predicate design. J Arthroplast 29:192–198. https://doi.org/10.1016/j.arth.2013.04.029
23. Dujardin FH, Mollard R, Toupin JM, Coblentz A, Thomine JM (1996) Micromotion, fit, and fill of custom made femoral stems designed with an automated process. Clin Orthop Relat Res 325:276–289
24. Saito J, Aslam N, Tokunaga K, Schemitsch EH, Waddell JP (2006) Bone remodeling is different in metaphyseal and diaphyseal-fit uncemented hip stems. Clin Orthop Relat Res 451:128–133. https://doi.org/10.1097/01.blo.0000224045.63754.a3
25. Vidalain JP (2011) Twenty-year results of the cementless Corail stem. Int Orthop 35:189–194. https://doi.org/10.1007/s00264-010-1117-2
26. Jacquot L, Bonnin MP, Machenaud A, Chouteau J, Saffarini M, Vidalain JP (2017) Clinical and radiographic outcomes at 25-30 years of a hip stem fully coated with hydroxylapatite. J Arthroplast. https://doi.org/10.1016/j.arth.2017.09.040
27. Flecher X, Pearce O, Parratte S, Aubaniac JM, Argenson JN (2010) Custom cementless stem improves hip function in young patients at 15-year followup. Clin Orthop Relat Res 468:747–755. https://doi.org/10.1007/s11999-009-1045-x
28. Pakos EE, Stafilas KS, Tsovilis AE, Vafiadis JN, Kalos NK, Xenakis TA (2015) Long term outcomes of total hip arthroplasty with custom made femoral implants in patients with congenital disease of hip. J Arthroplast 30:2242–2247. https://doi.org/10.1016/j.arth.2015.06.038
29. Colas S, Allalou A, Poichotte A, Piriou P, Dray-Spira R, Zureik M (2017) Exchangeable femoral neck (dual-modular) THA prostheses have poorer survivorship than other designs: a nationwide cohort of 324,108 patients. Clin Orthop Relat Res 475:2046–2059. https://doi.org/10.1007/s11999-017-5260-6
30. Bernstein DT, Meftah M, Paranilam J, Incavo SJ (2016) Eighty-six percent failure rate of a modular-neck femoral stem design at 3 to 5 years: lessons learned. J Bone Joint Surg Am 98:e49. https://doi.org/10.2106/JBJS.15.01082
31. Kwon YM, Khormaee S, Liow MH, Tsai TY, Freiberg AA, Rubash HE (2016) Asymptomatic pseudotumors in patients with taper corrosion of a dual-taper modular femoral stem: MARS-MRI and metal ion study. J Bone Joint Surg Am 98:1735–1740. https://doi.org/10.2106/JBJS.15.01325
32. Terrier A, Levrero Florencio F, Rüdiger HA (2014) Benefit of cup medicalization in total hip arthroplasty is associated with femoral anatomy. Clin Orthop Relat Res 472:3159–3165. https://doi.org/10.1007/s11999-014-3787-3
33. Boese CK, Jostmeier J, Oppermann J, Dargel J, Chang DH, Eysel P, Lechler P (2016) The neck shaft angle: CT reference value of 800 hips. Skelet Radiol 45:455–463. https://doi.org/10.1007/s00256-015-2314-2